The year 2019 in the *European Heart Journal – Cardiovascular Imaging*: part II

Bernard Cosyns (ORCID) [1]*, **Kristina H. Haugaa**[2], **Bernrhard Gerber**[3], **Alessia Gimelli**[4], **Leyla Elif Sade**[5], **Gerald Maurer**[6], **Bogdan A. Popescu**[7], **and Thor Edvardsen**[2]

[1]Cardiology, CHVZ (Centrum voor Hart en Vaatziekten), ICMI (In Vivo Cellular and Molecular Imaging) Laboratory, Universitair ziekenhuis Brussel, 101 Laarbeeklaan, Brussels 1090, Belgium; [2]Department of Cardiology, ProCardio Centre for Innovation, Oslo University Hospital, Rikshospitalet, Oslo Norway and Institute for clinical medicine, University of Oslo, Oslo, Norway; [3]Division of Cardiology, Department of Cardiovascular Diseases, Cliniques Universitaires St. Luc, Pôle de Recherche Cardiovasculaire (CARD), Institut de Recherche Expérimentale et Clinique (IREC), Université Catholique de Louvain, Av Hippocrate 10/2806, Brussels, Belgium; [4]Fondazione Toscana G. Monasterio, Pisa, Italy; [5]Department of Cardiology, Faculty of Medicine, Baskent University, Ankara, Turkey; [6]Division of Cardiology, Department of Internal Medicine II, Medical University of Vienna, Vienna, Austria; and [7]Department of Cardiology, University of Medicine and Pharmacy "Carol Davila"—Euroecolab, Emergency Institute for Cardiovascular Diseases "Prof. Dr. C. C. Iliescu", Sos. Fundeni 258, Sector 2, 022328 Bucharest, Romania

The *European Heart Journal – Cardiovascular Imaging* was launched in 2012 and has during these years become one of the leading multimodality cardiovascular imaging journal. The journal is now established as one of the top cardiovascular journals and is the most important cardiovascular imaging journal in Europe. The most important studies published in our Journal from 2019 will be highlighted in two reports. Part II will focus on valvular heart disease, heart failure, cardiomyopathies, and congenital heart disease. While Part I of the review has focused on studies about myocardial function and risk prediction, myocardial ischaemia, and emerging techniques in cardiovascular imaging.

Introduction

European Heart Journal – Cardiovascular Imaging has successfully consolidated as a multimodality journal during its first 8 years. It has now an important role as a significant resource for cardiologists, specialists in all imaging modalities, and other physicians working in the field of cardiovascular imaging. The tradition of highlighting the most important studies that were published in the last year is continued.[1,2] In two articles, we will summarize the most important papers from the journal in 2019. Part I has just been published.[3] Part II will focus on cardiomyopathies, congenital heart diseases, valvular heart diseases, and heart failure (HF).

One important assignment of *European Heart Journal – Cardiovascular Imaging* is to publish position papers, recommendations and expert consensus papers from the European Association of Cardiovascular Imaging (EACVI). The journal published recommendations and expert consensus papers in the field of cardiac imaging and also the best research presented at our conferences in 2019.[4–10]

These papers are commented on in more detail elsewhere in the two documents.

Cardiomyopathies

Castrini *et al.*[11] assessed the relation between the number of pregnancies and cardiac structure, function, and arrhythmic events in women with arrhythmogenic cardiomyopathy. They included 77 women with arrhythmogenic cardiomyopathy (43 probands and 34 arrhythmogenic cardiomyopathy mutation positive female relatives), 19 years after last pregnancy. The number of pregnancies was not associated with any measures of cardiac structure and function. Higher number of pregnancies did not seem to relate to a worse cardiac phenotype in women with arrhythmogenic cardiomyopathy.

Kobayashi *et al.*[12] compared the prognostic value of the myocardial performance index with other strain and remodelling indices in hypertrophic cardiomyopathy (HCM). They enrolled 126 patients

with HCM and 50 age- and sex-matched controls. They measured myocardial performance index, left ventricular (LV) global longitudinal strain, E/e′ ratio, and total left atrial global strain along with traditional measures. Time-based myocardial performance index was calculated from flow or tissue-based pulse wave Doppler as the (isovolumic-relaxation and contraction time)/systolic-time. They concluded that the time-based index was less predictive of outcome than strain or tissue Doppler indices. Left atrial global strain may be a promising prognostic marker in HCM.

Myocardial oxygenation is impaired in HCM patients with LV hypertrophy, and possibly in HCM gene carriers without LV hypertrophy. Grover *et al.*[13] studied whether these oxygenation changes are also associated with abnormalities in diastolic function or LV strain. They included 20 MYBPC3 gene-positive patients with LV hypertrophy, 18 MYBPC3 gene positive without LV hypertrophy, 11 gene negative siblings, and 11 normal controls. All subjects underwent 2D transthoracic echocardiography and cardiovascular magnetic resonance imaging (MRI) for assessment of ventricular volumes, mass, and myocardial oxygenation at rest and adenosine stress using the blood oxygen level-dependent technique. They found myocardial deoxygenation during stress in MYBPC3 HCM patients, even in the presence of normal LV diastolic function, LV global longitudinal strain, and LV wall thickness.

Pagourelias *et al.*[14] investigated the relationship between wall thickness and location, loading conditions and underlying pathological substrate with longitudinal and circumferential strain in a group of patients with HCM and cardiac amyloidosis. They included 30 patients with biopsy-proven cardiac amyloidosis and 50 patients with HCM matched for maximum wall thickness. Patients were investigated by cardiac magnetic resonance (CMR) and strain echocardiography. Results indicated that regional myocardial mechanics were differently influenced by local morphological parameters. While longitudinal strain was dominated by wall thickness, circumferential strain was more determined by location of hypertrophy and histology.

Esposito *et al.*[15] investigated regional LV patterns of longitudinal strain and base-to-apex behaviour of strain in treatment-naïve patients with Anderson–Fabry disease. They included 23 consecutive Anderson–Fabry patients at diagnosis and 23 healthy controls matched for age and sex. Results showed an early reduction of LV longitudinal strain, involving mainly LV basal myocardial segments. However, apical segments were not spared at time of diagnosis.

Binder *et al.*[16] compared right and LV parameters in patients with light chain (AL) and wild-type transthyretin amyloidosis (ATTRw) and evaluated their ability to predict cardiac outcome. They included 122 patients with cardiac amyloidosis, 62 with ATTRw, and 60 with AL. Baseline assessment included biventricular 2D speckle-tracking imaging parameters and patients were followed regularly. Results suggested different mechanisms underlying HF between ATTRw and AL, which may have substantial implications in particular in light of emerging therapies for both subtypes of cardiac amyloidosis. The study was commented in an editorial comment, highlighting the importance of correct diagnosis and the potential impact on pharmaceutical strategies.

Cho *et al.*[17] investigated the incidence of structural cardiac abnormalities and changes of cardiac geometry in highly trained university athletes and performed echocardiography in 1185 university athletes.

They found that abnormal LV geometry was not uncommon (13%) and concentric remodelling was the most common pattern of LV geometric change in young trained university athletes. Race, type of sport, and training time were significant predictors of abnormal LV geometry.

Van Der Bijl *et al.*[18] investigated the role of LV global longitudinal strain (GLS) as an early disease marker in genetic dilated cardiomyopathy (DCM). They investigated 115 individuals grouped according to positive or negative genotype and phenotype. Decreased LV global longitudinal strain discriminated genotype positive, phenotype negative individuals from normal controls, which may permit early institution of therapy for genetic DCM.

Dr Donal chaired the expert consensus document from the EACVI on Multimodality imaging in the diagnosis, risk stratification, and management of patients with dilated cardiomyopathies. The document provided recommendations for the use of multimodality imaging according to the clinical question. There remain some gaps in evidence on the impact of multimodality imaging on the management and the treatment of DCM patients where ongoing research is important.[6]

Several other studies evaluated genotype-phenotype relations in cardiomyopathies using CMR. Augusto *et al.*[19] evaluated phenotypes of 89 patients with DCM-associated mutations to evaluate if there would be specific imaging phenotypes which are associated with mutations with higher degree of arrhythmogenicity. They demonstrated that patients with filamin C (FLNC), and desmoplakin (DSP) mutations had had more extensive LV scar with a ring-like pattern in the majority of patients. They proposed that this pattern might be a diagnostic criterion to identify patients with higher risk of arrhythmia and LV arrhythmogenic cardiomyopathy (ALVC). Similarly, Segura-Rodríguez evaluated genotype-phenotype relations in arrhythmogenic right ventricular cardiomyopathy/dysplasia (ARVC/D). They demonstrated that patients with desmosomal mutations had different morphofunctional features from non-desmosomal mutations. In particular, right ventricular (RV) late gadolinium hyperenhancement (LGE) was more frequently observed in patients carrying a desmosomal mutation in comparison with the non-desmosomal and genotype-negative groups, although it did not reach statistical significance and that left circumferential sub-epicardial LGE was present in desmin mutations.[20] Also in ARVC/D, Jurlander *et al.*[21] evaluated the diagnostic yield of family screening in 286 relatives to proband diagnosed with definite ARVC. They reported a relatively low diagnostic yield of 7% of definite ARVC/D by task force criteria, with higher sensitivity of ECG, signal-averaged ECG, and Holter monitoring than imaging modalities. This suggests that initial evaluation of asymptomatic ARVC relatives should be performed by electrical abnormalities first.

In HCM, Ricci *et al.*[22] evaluated pulmonary blood volume index from first-pass perfusion imaging as quantitative biomarker of haemodynamic congestion. They demonstrated that increases in pulmonary blood volume index (PBVI) yield good diagnostic accuracy for the detection of diastolic dysfunction with elevated left atrial pressure (LAP) and that magnitude of pulmonary blood volume correlated with the severity of diastolic dysfunction and worsening functional capacity.

For amyloidosis diagnosis, multimodality imaging plays an important role. Jurcuţ *et al.*[23] published a review on multimodality imaging of

this disease while Nicol et al.[24] evaluated a diagnostic score of cardiac involvement in AL amyloidosis established by CMR using a combination of troponin T blood levels and two echo derived strain parameters resulting in very high sensitivity and specificity for identification of this disease.

In 20 female Fabry disease patients without cardiac symptoms, Imbriaco used positron emission tomography (PET)-mitral regurgitation (MR) to evaluated fasted fluorodesoxyglucose (FDG) glucose uptake and measure native T1 time. They demonstrated focal FDG uptake was present in segment with pseudonormalization of abnormal T1, which might represent an intermediate stage before development of myocardial fibrosis.[25] In 88 male patients with Becker muscular dystrophy, Marty et al.[26] performed comprehensive quantitative CMR with cine, tagging, T1, T2, and extracellular volum (ECV) measurements. They demonstrated reduced LV mass, ejection fraction, RV volumes, global circumferential strain higher myocardial dyssynchrony, and lower global native T1 and higher T2 and ECV measurements. This suggests that native T1 and T2 mapping could provide biomarkers related to inflammation and fibrosis processes that stratify disease severity in bone mineral density patients with a comparable sensitivity than quantitative contrast-enhanced CMR.

Werner et al. aimed to elucidate the potential role of longitudinal 2-Deoxy-2-18F-fluoro-D-glucose (18F-FDG) PET inflammation monitoring in a rat model of experimental autoimmune myocarditis. To this purpose, autoimmune myocarditis was induced in Lewis rats. Time course of disease was assessed by longitudinal 18F-FDG PET imaging.

After immunization, myocarditis rats revealed a temporal increase in 18F-FDG uptake (peaked at Week 3), which was followed by a rapid decline thereafter. Localization of CD68 positive cells was well correlated with *in vivo* 18F-FDG PET signalling as well as with *ex vivo* 18F-FDG autoradiography. CD44 positivity was primarily observed at tissue samples obtained at acute phase (i.e. at peak 18F-FDG uptake), while CD34-positive staining areas were predominantly identified in samples harvested at both sub-acute and chronic phases (i.e. at 18F-FDG decrease). The authors concluded that 18F-FDG PET imaging can provide non-invasive serial monitoring of cardiac inflammation in a rat model of acute myocarditis.[27]

Heart failure

Charisopoulou et al.[28] used 2D echocardiographic strain analysis to assess right atrial (RA) and RV mechanics and predict the need for RV mechanical support after left ventricular assist device (LVAD) implantation. Seventy advanced chronic HF patients received continuous-flow LVAD as a bridge to transplantation over an 18-month period. In LVAD recipients needing high ventricular assist device support, there was lower RA longitudinal strain and lower RV free wall longitudinal strain in addition to greater RV free wall mechanical delay. They concluded that RA and RV strain and dyssynchrony analysis have the potential to add incremental value to the pre-ventricular assist device-implantation assessment by conventional echo measurements.

Al Saikhan et al.[29] used 2D-speckle-tracking echocardiography to assess left atrial phasic function in patients with HF with preserved ejection fraction (HFpEF) and heart failure with mildly reduced ejection fraction (HFmrEF). They prospectively enrolled patients diagnosed with HF according to current European recommendations. Left atrial phasic function was worse in HFmrEF patients compared with those with HFpEF regardless of left atrial size, and independent of potential confounders. They attributed these differences to intrinsic left atrial myocardial dysfunction perhaps in relation to altered LV function.

Machino-Ohtsuka et al.[30] assessed the impact of LV diastolic function grade stratified by the updated 2016 echocardiographic algorithm (DD2016) on post-discharge outcomes in patients admitted for acute HF and compared with the previous 2009 algorithm (DD2009). The study included 481 patients hospitalized for acute decompensated HF. They found that despite simplification of the algorithm for LV diastolic function evaluation, the prognostic value of DD2016 for post-discharge cardiovascular events in HF patients was maintained and not compromised in comparison with DD2009.

Przewlocka-Kosmala et al.[31] explored the associations of global longitudinal strain and myocardial work parameters with the response of exercise capacity to spironolactone in HFpEF. They analysed 114 patients participating in the STRUCTURE study (57 randomized to spironolactone and 57 to placebo). Global constructive work as a measure of LV contractile response to exertion was a better determinant of exercise capacity in HFpEF than global longitudinal strain. Improvement in functional capacity during follow-up was associated with improvement in exertional increment of global constructive work.

Seo et al.[32] investigated the relationship between RV strain and adverse events in patients with DCM with sinus rhythm. They enrolled 143 DCM patients with sinus rhythm and performed echocardiography with RV strain. During 40 months of follow-up, adverse cardiovascular events developed in 21 patients (15%). RV free wall longitudinal strain was associated with a significant prognostic impact in DCM patients with sinus rhythm.

Several studies evaluated cardiac mechanics of different aetiologies of HF using multimodality imaging techniques. Rodriguez-Granillo evaluated the impact of cardiac compression by pectus excavatum using CMR, chest computed tomography (CT), and stress echocardiography. They demonstrated that exercise capacity and systolic and diastolic function were related to the severity of chest malformation and the degree of maximum compression over the right heart cavities.[33] Larsen evaluated regional myocardial work from strain by feature tracking CMR and non-invasive LV pressure in patients with reduced ejection fraction and left bundle branch block related to energy demand by FDG PET uptake demonstrating marked regional work heterogeneity with reduced work in septum compared to lateral wall in such left bundle branch block.[34] Agger et al.[35] used hyperpolarized MRI with 13C-pyruvate and echocardiography to study myocardial metabolism in a pig model of RV dysfunction induced by pulmonary banding. Similarly, Attard et al.[36] studied the translational regulation and energy metabolism in patients with pulmonary hypertension by metabolomics and 3D biomechanical modelling of the right ventricle from CMR images to computed regional wall stress. They demonstrated that wall stress was an independent predictor of all-cause mortality and that different metabolites pathways that reported on energy metabolism and cellular stress response including tRNA-specific modified nucleosides and fatty acid acylcarnitines were influenced by increased wall stress. In 167 consecutive patients with

HFpEF, Nitsche et al.[37] evaluated native T1 mapping and demonstrated that increased native T1 time ate the anterior RV insertion point was independently related with outcome and outcome and outperformed ECV as well as LGE by multivariable analysis.

Patients with non-ischaemic systolic HF often have reduced myocardial blood flow without significant coronary atherosclerosis. Likewise, patients with atrial fibrillation (AF) have reduced myocardial perfusion during AF compared with sinus rhythm. Byrne et al.[38] aimed to explore if there is an additive negative effect of AF during scan on the myocardial perfusion in patients with non-ischaemic systolic HF. To this purpose, they enrolled 114 patients with non-ischaemic systolic HF and 27 young healthy controls to a Rubidium-82 PET/CT perfusion scan (23 with AF during scan) at rest and after adenosine infusion. Patients with AF were older and more were men. Patients with AF had significantly lower myocardial flow reserve (MFR) than patients without and MFR remained significantly lower in the group with AF in an adjusted multivariable regression analysis. Furthermore, patients had lower MFR and highest coronary vascular resistance compared with controls. The authors concluded that patients with systolic HF had lower flow reserve than healthy controls and even lower MFR if they had AF during scan.

Nielsen et al.[39] evaluated in a porcine model of pulmonary congestion, the extravascular lung water (EVLW) and global end-diastolic volume (GEDV) by PET. The method was then applied in 35 HF patients and 9 healthy volunteers. The authors demonstrated that myocardial perfusion imaging using a single dynamic $15O-H_2O-PET$ examination can be applied to measure EVLW and GEDV, and hence, quantitatively and non-invasively assess the degree of pulmonary congestion and cardiac filling volumes. Hence, this study demonstrates that EVLW and GEDV can be estimated quantitatively without additional examinations or radiation in patients subjected to myocardial perfusion examination by $15O-H_2O-PET$. Thus, EVLW and GEDV should be assessed for their prognostic value and evaluated as a therapeutic target in HF patients.

Congenital heart disease

Ewen et al.[40] conducted an echocardiography study including 69 patients with intraoperatively confirmed unicuspid aortic valve (UAV) in order to determine echocardiographic diagnostic criteria. They compared the findings with bicuspid aortic valves (BAV) and tricuspid aortic valves (TAV) as confirmed by surgical exploration. They defined a single commissural attachment zone, rounded leaflet-free edge on the opposite side of the commissural attachment zone, eccentric valvular orifice during systole, and patient age <20 years with mean transvalvular gradient >15 mmHg as diagnostic criteria. The minor criteria were defined as an associated thoracic aortopathy and age <40 years. Three out of the four major criteria or two out of the four major criteria and one minor criterion were met in all patients with UAV. The proposed echocardiographic score system was specific (98–100%) and sensitive (95–100%) to distinguish UAV from BAV and TAV.

Kamphuis et al.[41] assessed intraventricular viscous energy loss (EL) and proportionality to kinetic energy (KE) in 30 Fontan patients using 4D flow MRI and compared with 15 healthy controls. To provide some insights into the disturbed intra-cardiac flow patterns and help to better understand the reasons of circulatory failure which is the main cause of mortality in these patients. Patients were grouped into two groups for comparison to each other by: (i) concordance or discordance: Concordant inflow-to-outflow (inflow of blood into the same ventricle from which the blood is ejected into the aorta) or discordant inflow-to-outflow [inflow of all (or part of) the blood entering a ventricle, which leaves that ventricle through a ventricular septal defect to the aorta], and (ii) systemic LV vs. systemic RV. Fontan patients with discordant inflow-to-outflow had significantly elevated EL compared with Fontan patients with concordant inflow-to-outflow; EL was not significantly different between Fontan patients with a systemic LV vs. a systemic RV. Fontan patients showed disproportionate intraventricular EL relative to produced KE most likely due to viscosity-induced frictional forces. The use of EL parameters as a reflector of higher flow–structure interaction in Fontan patients, by 4D flow MRI, seems useful in early detection of circulatory failure.

Grotenhuis et al.[42] studied LV remodelling in long-term survivors after the arterial switch operation for transposition of the great arteries in a prospective study by CMR including myocardial perfusion, LGE and T1 relaxometry in addition to echocardiography with strain analyses. After the operation, LV EF (ejection fraction) was normal but volumes were increased, longitudinal strain decreased while circumferential strain increased as a possible compensatory mechanism. Native T1 times were mildly higher, however, no scar by LGE or no perfusion defect were detected in children and adolescents after arterial switch operation in keeping with excellent long-term outcome of these patients.

Diller et al.[43] used machine learning algorithms in assessment of patients with systemic RV [i.e. in transposition of great arteries (TGA) after arterial switch operation or congenitally corrected (ccTGA)] trained on routine echocardiographic datasets. In addition, they evaluated the ability of deep learning for delineation and segmentation of the systemic ventricle in 132 patients and compared these with controls. The U-Net architecture model correctly identified the systemic ventricle in all individuals and achieved a high performance in segmenting the systemic ventricle. On combined cine-loop frames, the algorithm correctly identified 100% of the TGA, 100% of the normal hearts, and 93.8% of the ccTGA hearts in comparison to human expert readings. This study underlines the promising value of machine learning algorithms, trained on routine echocardiographic datasets for making diagnoses even in complex congenital heart disease.

In congenital heart disease, several studies evaluated the predictors of reduced exercise capacity. In 235 patients with repaired tetralogy of Fallot, Gnanappa evaluated the effect of RV dilatation of LV function and RV–LV interaction and changes after pulmonary valve replacement. They documented that patients with severe TV dilatation had increased net pulmonary forward flow, LV stroke, and diastolic volume, indicating that increased LV preload appears to overcome diastolic septal shift allowing to maintain preserved exercise capacity in these patients with severe RD dilatation.[44] Similarly, Rashid et al.[45] correlated CMR and with cardiopulmonary exercise testing, to evaluate which parameter correlates best with reduction of exercise performance. They identified CMR-derived RVEF and RV stroke volume index (SVi) but not RV dilatation as independent predictors of cardiopulmonary

exercise testing (CPET) performance. This suggests that detection of reductions in RV systolic function in patients with significant PR and varying degrees of RV dilatation may improve the identification of patients at elevated risk of adverse cardiac events and improve the selection of patients for PVR. Finally, Cochet et al.[46] studied correlates of focal scar and diffuse fibrosis in such tetralogy of Fallot (TOF) patients. They found that scar area and LV native T1 were independent correlates of ventricular arrhythmia, while RVEF was not. Patients with history of pulmonary valve replacement (PVR) showed larger scars on RV outflow tract but shorter LV and RV native T1.

Valvular heart disease

Garg et al.[47] investigated the association of aortic (AVC) and mitral annular calcification (MAC) with the risk of developing clinical peripheral arterial disease (PAD). AVC and MAC were measured on cardiac computed tomography in 6778 Multi-Ethnic Study of Atherosclerosis (MESA) participants without baseline PAD. In this study, 907 patients (13.3%) had AVC and 640 (9.4%) had MAC. Participants with baseline MAC were older, less likely to be physically active or a current smoker, and more likely to be female. The presence of MAC was associated with a higher risk of developing clinical PAD in women. No significant association was detected between the presence of AVC and PAD. Females in this cohort had a lower rate of traditional PAD risk factors, namely diabetes and smoking, compared with men. The presence of valvular calcification may have captured some of the risk in women not accounted for by these risk factors.

Stella et al.[48] tested the accuracy and reproducibility of aortic annular measurements obtained from 3D echocardiographic manual and semi-automated software analyses in comparison to multislice computed tomography (MSCT), as the gold standard, in 171 patients before transcatheter aortic valve implantation (TAVI). Both 3D methods underestimated the MSCT measurements, but semi-automated measurements showed narrower limits of agreement and lesser bias than manual measurements with small underestimations in general, except for the minor diameter. The deviation was mainly related to calcification and elliptic shape of the annulus. Both 3D-TOE (transoesophageal echocardiography) measurements moderately agreed with MSCT for valve sizing (Kappa = 0.5). The authors concluded that 3D-TOE semi-automated analysis is reliable and can be used in clinical practice as an alternative to MSCT possibly by applying a correction factor of overestimation with respect to the manufacturer-recommended CT-based sizing algorithm. Echocardiographic measurements of LV outflow tract (LVOT) and aortic root have also been tested against MSCT for their accuracy and reproducibility. In 51 patients, Visby et al.[49] found that both 2D/3D TTE underestimated the areas compared with MSCT; however, 3D TTE areas were more closer to MSCT derived areas than 2D measurements. Feasibility with 3D was 76–79% (lowest for the annulus) less than the feasibility with 2D (88–90%). However, the reproducibility of LVOT and aortic annulus measurements by 3D TTE was better than 2D TTE, yet intraobserver coefficient of variation was 9%, and even higher (18–20%) at day-to-day re-test by 3D TTE. Boraita et al.[50] examined BAV behaviour in 41 elite athletes and compared those with elite athletes having TAV and also with non-athlete BAV patients. In the study population of 5136 elite athletes, the prevalence of BAV was 0.8%, similar to the general population. Proximal ascending aorta, sinus of Valsalva, and sinotubular junction were larger in both BAV groups (elite athletes and non-athletes) compared with athletes having TAV. The progression of the disease was assessed in 16 elite athletes with BAV at two cardiac evaluations separated by more than 3 years. The authors concluded that BAV elite athletes, with mild-to-moderately dilated aortas, may engage in high dynamic cardiovascular exercises without adverse consequences, although an echocardiographic follow-up is recommended given the high inter-individual variability seen in aortic diameters. Padang et al.[51] investigated the prevalence and the characteristics of mitral valve prolapse (MVP) that coexists with BAV and TAV in a retrospective study. The community prevalence of MVP-BAV was comparable with MVP-TAV (2.7% vs. 3.4%). Although posterior leaflet prolapse was the most common MVP phenotype, anterior-leaflet prolapse was twice as prevalent in MVP-BAV than in MVP-TAV patients. An extreme phenotype of giant anterior-MVP was observed in 14% of MVP-BAV patients; with male predominance, characterized by diminutive posterior mitral leaflet, high prevalence of mitral and aortic regurgitation (AR), and high rate of mitral repair failure.

A study by Vollema et al.[52] elaborated on LV reverse remodelling and mechanical changes over time (at 1, 2, and 5 years) after aortic valve surgery in aortic stenosis (AS, n = 132) and AR (n = 79). Before surgery, LV mass index was larger in AR patients than AS patients, GLS was moderately impaired in both groups. After surgery, both groups showed LV mass regression, although more pronounced in AR patients. LV GLS improved in both groups over the long term, but GLS initially declined in AR patients while in AS patients it remained initially stable. Distinct patterns in LV reverse remodelling and mechanics point out the differences in myocardial response to pressure overload relief in AS and a combination of pressure and volume overload relief in AR. Of note, the authors did not compute GLS normalized to end-diastolic volume (strain/EDV) to correct for the volume dependency of deformation in patients with AR. RulE out Transcatheter aOrtic valve thRombosis with post Implantation Computed tomography (RETORIC) study was a prospective, single-centre, observational study, which included asymptomatic patients after TAVI with CoreValve. From the RETORIC study cohort (117 patients with pre- and post-CTA (computed tomography angiography)) a substudy showed that the prevalence of subclinical leaflet thrombosis (SLT) was 25.6% and associated with diminished LV reverse remodelling (LV mass reduction <20%). Impaired LV reverse remodelling remained an independent predictor of adverse clinical outcomes (death and HF hospitalization) during a mean follow-up duration of 2.6 years. As a result, SLT and LV reverse remodelling are proposed as novel imaging targets for post-TAVI patient management.[53]

Saeed et al.[54] conducted a retrospective study to assess the survival benefit of aortic valve replacement (AVR) in patients with normal flow [flow rate (FR) = stroke volume/ejection time rate; >200 mL/s], low gradient (<40 mmHg), severe AS (valve area <1 cm^2), and normal EF (>50%). The outcome measure was all-cause mortality over a mean follow-up of 3.2 ± 1.8 years. They found that AVR (n = 125) was associated with significantly lower risk of death compared with those conservatively treated (n = 151). Not having

AVR was associated with a 6.3-fold higher risk of all-cause mortality. The risk of death due to not having AVR was >1.5 times higher in the FR defined model than in the model where flow was defined by SVi $\geq$35 mL/m^2. However, one should be cautious about the superiority of FR over SVi as the study was not powered and designed for this comparison. Nevertheless, the findings underscore that an important proportion of patients with normal flow-low gradient indeed have true-severe AS and benefit from AVR. Kimura et al.[55] defined distinct features of ischaemic MR in acute myocardial infarction (MI). The investigators used a new 4D-imaging software to quantify dynamically mitral apparatus and LV characteristics in 174 patients with and without MR after first MI and in chronic stage in 44 patients. Unlike chronic ischaemic MR, in patients with acute ischaemic MR, mitral annular, valvular, and sub-valvular dynamics were largely maintained throughout the cardiac cycle. Only modest enlargement and flattening of the annulus, and tenting of the leaflets linked to MR severity were observed. Conversely, papillary muscle (PM) displacement was radically different: More apical displacement in chronic ischaemic MR vs. wider PM angle in acute ischaemic MR. Separation and excess angulation of PMs imposing an acute lateral traction on the leaflets were responsible of acute ischaemic MR, as a result of regional wall motion abnormality without apparent global LV remodelling. Distinct features for acute ischaemic MR complicating acute MI provide insights into therapeutic strategies.

Ikenaga et al.[56] investigated morphological changes in 41 patients who underwent repeat intervention for recurrent MR after initial 478 consecutive MitraClip procedures, by using 3D-transoesophageal echocardiography. Worsening prolapse at the clip site was the most frequent cause of recurrent MR among primary MR patients followed by leaflet tear at the clip site. In secondary MR patients, however, the progression of LV remodelling with increasing leaflet tenting was the most frequent cause of recurrence. Number of clips was not a predictor. Meanwhile, device detachment was observed more frequently in patients with primary MR.

Pimor et al.[57] investigated predictors of postoperative cardiovascular events after mitral valve surgery for primary MR. They performed unbiased clustering analysis using dense phenotypic data to identify phenotypically distinct categories of 122 patients. Three phenogroups out of the heterogeneous primary MR population were created using a dedicated phenomapping algorithm in 122 patients. The primary endpoint events were pre-defined as post-operative death, AF, stroke, and re-hospitalization. These phenogroups had different prognosis, suggesting different risk profiles. Machine learning tools are promising to cluster and merge large amount with echocardiographic parameters to develop patient-tailored follow-up after MVR.

A comprehensive review elaborating on the evolving role of CMR in primary mitral regurgitation has been published. The role of CMR in an integrated surveillance and surgical timing is discussed in the light of the current evidence in the review.[58]

Utsunomiya et al.[59] studied 76 consecutive patients with reduced LV EF (25.4–44.6%) undergoing MitraClip for functional MR with central ($n = 39$) and eccentric ($n = 37$) jets selected among EVERST and COAPT trial populations (Figure 1). The authors examined the mechanisms of improvement in MR by MitraClip according to functional MR subtypes and demonstrated fundamental differences between eccentric and central functional MR. The difference in tethering angle between anterior and posterior mitral leaflets and the posterior PM-leaflet distance was strongly associated with MR severity in eccentric MR, whereas the tenting volume was the only independent predictor of MR severity in central MR. As a result, different responses to the clip procedure occurred in these two subgroups. In central MR, improvement after MitraClip therapy was associated with the reduction in antero-posterior diameter and improved MV coaptation, whereas it was mainly associated with the improvement of asymmetrical leaflet tethering pattern in eccentric functional MR. The authors concluded that detecting the exact location of the pseudo-prolapse of anterior mitral leaflet and firstly trying to capture the tethered posterior mitral leaflet correctly, is of great importance during MitraClip placement in eccentric functional MR. If the functional MR jet is central, the importance of a reduction in antero-posterior diameter and increase in coaptation area should be taken into consideration during the procedure. Brouwer et al.[60] investigated LV remodelling patterns after MitraClip implantation with serial echocardiography before, 1 and 6 months after implantation in 79 patients (81% having severe functional MR). Sustained reduction of MR $\leq$2 was observed in 83% of the patients, reverse remodelling (decrease in EDV >15%) occurred in 51%, adverse remodelling (>10% increase in EDV) occurred in 8% of the patients and no remodelling in the remaining. High systolic pulmonary artery pressure was the only independent determinant of LV remodelling. Mortality rate was higher in patients having adverse remodelling than patients having reverse remodelling over a period of 32 ± 16 months. Whether assessment of contractile reserve with stress echocardiography can better predict the development of adverse remodelling post-MitraClip was not investigated. The study also falls short to make conclusions about the effect of scar on LV remodelling given the small number of patients in the CMR subgroup. Akin to the previous study, Cimino et al.[61] sought to describe the incidence and determinants of LV reverse remodelling at 6 months of follow-up after MitraClip implantation in 41 patients with functional MR and reduced LV EF. Mean EF was 29 ± 11% and EDVi was 96 ± 24 as assessed by 3D echocardiography. At 6 months of follow-up, they found that patients presenting with higher LV volumes, logistic scores, and pulmonary artery systolic may not benefit from the procedure in terms of LV reverse remodelling despite a significant reduction of MR. The authors related the non-reverse remodelling to afterload mismatch. These findings might help to better select MitraClip candidates or to adopt additional corrective measures as well as intensified medical treatment. Faletra et al.[62] have published a comprehensive review in the journal providing the details of the peculiar aspects of mitral annulus in the light of 3D echocardiography as well as CT and CMR comparatively with anatomical and pathological specimens. The review provides rich and detailed descriptions about mitral annulus and surrounding structures and discussed clinical implications.

With increasing awareness of the impact of tricuspid regurgitation (TR) on prognosis and new percutaneous interventions on tricuspid valve, TR has been the focus of intensive research by means of 3D echocardiography. Santoro et al.[63] examined the prognostic impact of severe TR in subgroups defined as severe, massive, and torrential according to the recent classification scheme in 249 patients over 313 ± 103 days. Because of the retrospective design of the study only a semi-quantitative parameter, the vena contracta width, was used for the assessment of TR severity. The groups of patients with

massive/torrential TR had significantly higher rates of cardiovascular mortality than those with severe TR. In terms of different aetiologies, TR associated with pulmonary hypertension due to lung disease or primary pulmonary hypertension portended the worst prognosis, while TR due to annulus dilation without pulmonary hypertension and TR due to lead interference appeared more benign, unless overlooked due to low number of patients in the subgroups. Importantly, not all the 'severe' grades showed the same outcome. These findings are important to refine risk stratification for mortality and recurrent HF admissions as well as for setting the targets for new therapeutic approaches for patients who are too sick to be operated on. Of note, definite cut-offs still remain to be defined. Amano et al.[64] reported important findings about TR from the Contemporary Outcomes after Surgery and Medical Treatment in Patients with Severe Aortic Stenosis and results (CURRENT AS) Registry that enrolled 3815 consecutive patients with severe AS. There were 628 patients with moderate or severe TR (TR group) and 3187 patients with no or mild TR (no TR group). The 5-year freedom rate from the primary outcome (aortic valve-related death or hospitalization due to HF) was significantly lower in the TR group than in the no TR group, even after adjusting for confounders. An association between clinically significant TR and poor long-term outcome was observed in patients whether they underwent AVR or not. In addition, tricuspid

annuloplasty at the time of AVR did not have an impact on the primary outcome in patients with clinically significant TR. The lack of benefit is likely due to multiple associated factors (e.g. severe LV diastolic dysfunction, mitral valve diseases, pulmonary hypertension, and/or AF) that persist in these patients, even if tricuspid annuloplasty is performed. A randomized study is required to investigate whether tricuspid annuloplasty can improve outcome in patients with severe AS and clinically significant TR. Importantly, TR was only semi-quantitatively assessed in this registry. Another study, from Nassif et al.[65] aimed to develop a prediction model to identify patients with residual moderate/severe TR after percutaneous atrial septal defect (ASD) closure, because functional TR frequently co-exists due to RV volume overload and does not necessarily regress after closure of ASD or recurs. In this study, persistent moderate/severe TR was observed in 47% of the patients, by TTE with semi-quantitative assessment, 6 months after successful ASD closure ($n = 172$). The investigators proposed a risk score system to predict moderate/severe TR at 6 months of follow-up, including age >60 years, RV end-diastolic area ≥ 10 cm^2/m^2, and TAPSE ≤ 23 mm, each was assigned 1 point, and RV systolic pressure ≥ 44 mmHg assigned 2 points. Note that AF was not part of the score system because of its strong association with RA size. The probability of post-closure TR linearly increased from 10% with a score of 1 to almost 100% with a
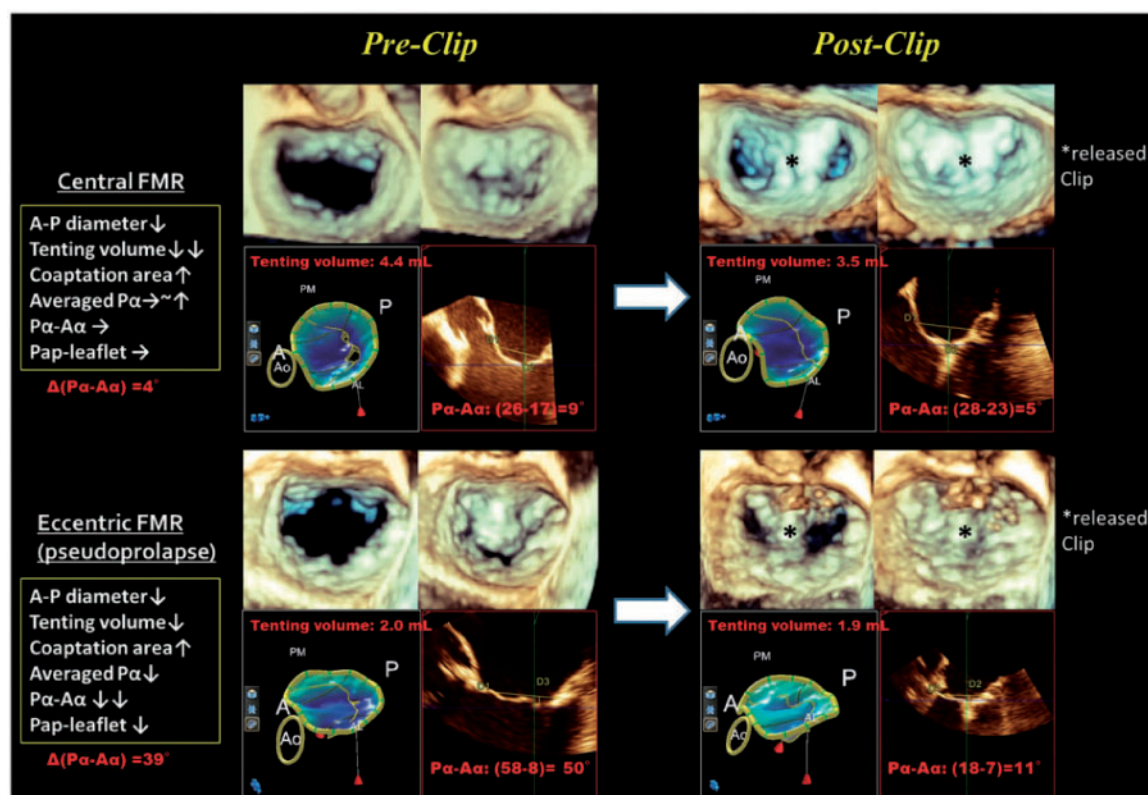

Figure 1 3D MV images and analyses pre- and post-clip. Compared with central FMR, eccentric FMR showed a greater improvement of asymmetrical tethering pattern but less prominent reduction of tenting volume. A, anterior; Aa, averaged tethering angle of anterior mitral leaflet; AL, anterolateral; IAS, interatrial septum; P, posterior; Pa, averaged tethering angle of posterior mitral leaflet; Pap, papillary muscle; PM, posteromedial. Pa-Aa means the difference in averaged tethering angle between anterior mitral leaflet (AML) and posterior mitral leaflet (PML). From Ref.[59]

cumulative score of 5. Patients with persistent significant TR at 6-month post-closure follow-up had higher rates of mortality and hospitalization for HF during long-term FU. These findings implicate that decreasing functional TR should be among the targets of ASD closure. Accordingly, for those in whom TR regression is unlikely, one can make the best decision regarding the intervention to ASD and TR. Finally, Faletra *et al.*[66] published a comprehensive review describing the anatomy of TV and surrounding structures by computed tomography, CMR, 2D/3D transthoracic echocardiography, and 2D/3D transoesophageal echocardiography emphasizing strengths and weaknesses of each of these imaging tools. Koo *et al.*[67] compared retrospectively the diagnostic accuracy of cardiac CT with that of echocardiography for the detection of MVP on a scallop-by-scallop basis, using surgical inspection as a reference standard. They enrolled 145 patients who underwent surgical MVP repair or replacement and preoperative cardiac CT. The prolapsed scallop was localized using cardiac CT and echocardiography according to the Carpentier method. The per-scallop sensitivity and specificity of each method were compared, using surgical inspection as a reference standard. Surgically, MVP was confirmed in 26% scallops. The per-scallop sensitivity of cardiac CT was lower than that of echocardiography (80% vs. 87%, *P* = 0.004), with similar specificity (both 95%). In particular, CT underestimated the extent of MVP in 31 patients and echocardiography in 22 patients. The authors concluded that cardiac CT provides a feasible method for localizing MVP on a per-scallop basis, but it may underestimate the extent of prolapsed scallop compared with echocardiography, particularly in patients with multiple-scallop lesions.

In valve disease, Dux-Santoy *et al.*[68] evaluated differences in aortic arch flow dynamics using 4D flow CMR between 111 patients with bicuspid valve, 21 age-matched tricuspid aortic valve patients with dilated arch, and 24 healthy volunteers. They observed that proximal aortic arch dilatation in bicuspid valve disease was associated with increased rotational flow, male gender, and AS, supporting the role of flow in aortic dilation in bicuspid disease. Hwang *et al.*[69] evaluated changes of native T1 times indicating myocardial fibrosis after AVR for severe AS. They found that that native T1 significantly decreased 1 year after AVR, which was associated with LV mass regression and systolic function improvement. Mortensen *et al.*[70] evaluated aortic growth rate in 91 patients with Turner syndrome over a mean follow-up of 5.7 years and compared them with 67 healthy female age-matched controls. Their study demonstrated that aortic growth rates in adult women with Turner syndrome were similar to or smaller than in healthy female controls when widely treated for clinical hypertension except in the presence of bicuspid valve or coarctation and that spontaneous aortic dissection was rare in bicuspid aortic valve.

The knowledge of normal reference values and of measurement variability is of paramount importance for measurements. In particular, there is a lack of normal values in the paediatric population. Therefore, Van Der Ven *et al.*[71] (PubMed ID: 31280290) reported volumetric CMR reference measurement for children aged 0–18 years in a lard multicentre cohort. Similarly, normal ranges for left atrial strain and strain rate by CMR were published by Truong et al. and Pathan et al. evaluated the intervendor and intramodality variability between CMR and TTE of this important biomarker.[72,73] In line with such automated measurements Raisi-Estabragh *et al.*[74] published

a review article on CMR Radiomics, a new image texture analysis technique allowing extract image features from pixel histograms to allow automated volume segmentations feature selection model building and advanced differentiation of myocardial disease states from machine learning algorithms.

Evaluation of large clinical databases by CMR has allowed to identify new risk markers. In the UK biobank analysing 4590 patients, Van Hout *et al.*[75] performed complete body composition MRI with anthropomorphic evaluation of subcutaneous and visceral fat and related them to LV volumes and function, demonstrating that visceral but not general obesity was related with smaller LV cardiac volumes and subclinical lower systolic function. In the MESA study in 2338 participants, Lim *et al.*[76] (PubMed ID: 31356656) evaluated longitudinal changes of left atrial volume in function and identified that increase in left atrial volumes and decrease in left atrial function was associated with incident AF and better prediction of AF risk. Anand *et al.*[77] in 7594 patients in the Canadian Alliance for Healthy Hearts and Minds Cohort (CAHHM) Study evaluated cardiac risk score, namely the INTERHEART risk score and the Framing ham risk score to predict risk of carotid vessel intraplaque haemorrhage and silent brain ischaemia detected by MR imaging.

Conflict of interest: none declared.

References

1. Edvardsen T, Haugaa KH, Petersen SE, Gimelli A, Donal E, Maurer G *et al.* The year 2018 in the *European Heart Journal – Cardiovascular Imaging*: part I. *Eur Heart J Cardiovasc Imaging* 2019;**20**:858–65.
2. Cosyns B, Haugaa KH, Gerber BL, Gimelli A, Donal E, Maurer G *et al.* The year 2018 in the *European Heart Journal - Cardiovascular Imaging*: part II. *Eur Heart J Cardiovasc Imaging* 2019;**20**:1337–44.
3. Edvardsen T, Haugaa KH, Petersen SE, Gimelli A, Donal E, Maurer G *et al.* The year 2019 in the *European Heart Journal—Cardiovascular Imaging*: part I. *Eur Heart J Cardiovasc Imaging* 2020;doi:10.1093/ehjci/jeaa259/5905662
4. Petersen SE, Khanji MY, Plein S, Lancellotti P, Bucciarelli-Ducci C. European Association of Cardiovascular Imaging expert consensus paper: a comprehensive review of cardiovascular magnetic resonance normal values of cardiac chamber size and aortic root in adults and recommendations for grading severity. *Eur Heart J Cardiovasc Imaging* 2019;**20**:1321–31.
5. Cardim N, Dalen H, Voigt J-U, Ionescu A, Price S, Neskovic AN *et al.* The use of handheld ultrasound devices: a position statement of the European Association of Cardiovascular Imaging (2018 update). *Eur Heart J Cardiovasc Imaging* 2019;**20**:245–52.
6. Donal E, Delgado V, Bucciarelli-Ducci C, Galli E, Haugaa KH, Charron P, *et al.*; 2016–18 EACVI Scientific Documents Committee. Multimodality imaging in the diagnosis, risk stratification, and management of patients with dilated cardiomyopathies: an expert consensus document from the European Association of Cardiovascular Imaging. *Eur Heart J Cardiovasc Imaging* 2019;**20**:1075–93.
7. Magne J, Cosyns B, Popescu BA, Carstensen HG, Dahl J, Desai MY *et al.* Distribution and prognostic significance of left ventricular global longitudinal strain in asymptomatic significant aortic stenosis: an individual participant data meta-analysis. *JACC Cardiovasc Imaging* 2019;**12**:84–92.
8. Magne J, Bharucha T, Cikes M, Galderisi M, Price S, Sade LE *et al.* EuroEcho 2019: highlights. *Eur Heart J Cardiovasc Imaging* 2020;**21**:469–78.
9. Rodriguez-Palomares JF, Edvardsen T, Almeida AG, Petersen SE. EuroCMR 2019 highlights. *Eur Heart J Cardiovasc Imaging* 2020;**21**:127–31.
10. Hyafil F, Jaber WA, Neglia D. Highlights of the 14th international conference on nuclear cardiology and cardiac computed tomography. *Eur Heart J Cardiovasc Imaging* 2020;**21**:1–9.
11. Castrini AI, Lie ØH, Leren IS, Estensen ME, Stokke MK, Klæboe LG *et al.* Number of pregnancies and subsequent phenotype in a cross-sectional cohort of women with arrhythmogenic cardiomyopathy. *Eur Heart J Cardiovasc Imaging* 2019;**20**:192–8.
12. Kobayashi Y, Moneghetti KJ, Bouajila S, Stolfo D, Finocchiaro G, Kuznetsova T *et al.* Time based versus strain based myocardial performance indices in hypertrophic cardiomyopathy, the merging role of left atrial strain. *Eur Heart J Cardiovasc Imaging* 2019;**20**:334–42.

13. Grover S, Lloyd R, Perry R, Lou PW, Haan E, Yeates L *et al.* Assessment of myocardial oxygenation, strain, and diastology in MYBPC3-related hypertrophic cardiomyopathy: a cardiovascular magnetic resonance and echocardiography study. *Eur Heart J Cardiovasc Imaging* 2019;**20**:932–8.

14. Pagourelias ED, Mirea O, Vovas G, Duchenne J, Michalski B, Van Cleemput J *et al.* Relation of regional myocardial structure and function in hypertrophic cardiomyopathy and amyloidois: a combined two-dimensional speckle tracking and cardiovascular magnetic resonance analysis. *Eur Heart J Cardiovasc Imaging* 2019;**20**:426–37.

15. Esposito R, Galderisi M, Santoro C, Imbriaco M, Riccio E, Maria Pellegrino A *et al.* Prominent longitudinal strain reduction of left ventricular basal segments in treatment-naïve Anderson-Fabry disease patients. *Eur Heart J Cardiovasc Imaging* 2019;**20**:438–45.

16. Binder C, Duca F, Stelzer PD, Nitsche C, Rettl R, Aschauer S *et al.* Mechanisms of heart failure in transthyretin vs. light chain amyloidosis. *Eur Heart J Cardiovasc Imaging* 2019;**20**:512–24.

17. Cho JY, Kim KH, Rink L, Hornsby K, Park H, Park JH *et al.* University athletes and changes in cardiac geometry: insight from the 2015 Gwangju Summer Universiade. *Eur Heart J Cardiovasc Imaging* 2019;**20**:407–16.

18. Van Der Bijl P, Bootsma M, Hiemstra YL, Ajmone Marsan N, Bax JJ, Delgado V. Left ventricular 2D speckle tracking echocardiography for detection of systolic dysfunction in genetic, dilated cardiomyopathies. *Eur Heart J Cardiovasc Imaging* 2019;**20**:694–9.

19. Augusto JB, Eiros R, Nakou E, Moura-Ferreira S, Treibel TA, Captur G *et al.* Dilated cardiomyopathy and arrhythmogenic left ventricular cardiomyopathy: a comprehensive genotype-imaging phenotype study. *Eur Heart J Cardiovasc Imaging* 2020;**21**:326–36.

20. Segura-Rodríguez D, Bermúdez-Jiménez FJ, Carriel V, López-Fernández S, González-Molina M, Oyonarte Ramírez JM *et al.* Myocardial fibrosis in arrhythmogenic cardiomyopathy: a genotype-phenotype correlation study. *Eur Heart J Cardiovasc Imaging* 2020;**21**:378–86.

21. Jurlander R, Mills HL, Espersen KI, Raja AA, Svendsen JH, Theilade J *et al.* Screening relatives in arrhythmogenic right ventricular cardiomyopathy: yield of imaging and electrical investigations. *Eur Heart J Cardiovasc Imaging*. 2020;**21**:175–82.

22. Ricci F, Aung N, Thomson R, Boubertakh R, Camaioni C, Doimo S *et al.* Pulmonary blood volume index as a quantitative biomarker of haemodynamic congestion in hypertrophic cardiomyopathy. *Eur Heart J Cardiovasc Imaging* 2019;**20**:1368–76.

23. Jurcuţ R, Onciul S, Adam R, Stan C, Coriu D, Rapezzi C *et al.* Multimodality imaging in cardiac amyloidosis: a primer for cardiologists. *Eur Heart J Cardiovasc Imaging* 2020;**21**:833–44.

24. Nicol M, Baudet M, Brun S, Harel S, Royer B, Vignon M *et al.* Diagnostic score of cardiac involvement in AL amyloidosis. *Eur Heart J Cardiovasc Imaging* 2020;**21**:542–8.

25. Imbriaco M, Nappi C, Ponsiglione A, Pisani A, Dell'Aversana S, Nicolai E *et al.* Hybrid positron emission tomography-magnetic resonance imaging for assessing different stages of cardiac impairment in patients with Anderson-Fabry disease: AFFINITY study group. *Eur Heart J Cardiovasc Imaging* 2019;**20**:1004–11.

26. Marty B, Gilles R, Toussaint M, Béhin A, Stojkovic T, Eymard B *et al.* Comprehensive evaluation of structural and functional myocardial impairments in Becker muscular dystrophy using quantitative cardiac magnetic resonance imaging. *Eur Heart J Cardiovasc Imaging* 2019;**20**:906–15.

27. Werner RA, Wakabayashi H, Bauer J, Schütz C, Zechmeister C, Hayakawa N *et al.* Longitudinal 18F-FDG PET imaging in a rat model of autoimmune myocarditis. *Eur Heart J Cardiovasc Imaging* 2019;**20**:467–74.

28. Charisopoulou D, Banner NR, Demetrescu C, Simon AR, Haley SR. Right atrial and ventricular echocardiographic strain analysis predicts requirement for right ventricular support after left ventricular assist device implantation. *Eur Heart J Cardiovasc Imaging* 2019;**20**:199–208.

29. Al Saikhan L, Hughes AD, Chung WS, Alsharqi M, Nihoyannopoulos P. Left atrial function in heart failure with mid-range ejection fraction differs from that of heart failure with preserved ejection fraction: a 2D speckle-tracking echocardiographic study. *Eur Heart J Cardiovasc Imaging* 2019;**20**:279–90.

30. Machino-Ohtsuka T, Seo Y, Ishizu T, Hamada-Harimura Y, Yamamoto M, Sato K *et al.* Clinical utility of the 2016 ASE/EACVI recommendations for the evaluation of left ventricular diastolic function in the stratification of post-discharge prognosis in patients with acute heart failure. *Eur Heart J Cardiovasc Imaging* 2019;**20**:1129–37.

31. Przewlocka-Kosmala M, Marwick TH, Mysiak A, Kosowski W, Kosmala W. Usefulness of myocardial work measurement in the assessment of left ventricular systolic reserve response to spironolactone in heart failure with preserved ejection fraction. *Eur Heart J Cardiovasc Imaging* 2019;**20**:1138–46.

32. Seo J, Jung IH, Park JH, Kim GS, Lee HY, Byun YS *et al.* The prognostic value of 2D strain in assessment of the right ventricle in patients with dilated cardiomyopathy. *Eur Heart J Cardiovasc Imaging* 2019;**20**:1043–50.

33. Rodriguez-Granillo GA, Raggio IM, Deviggiano A, Bellia-Munzon G, Capunay C, Nazar M *et al.* Impact of pectus excavatum on cardiac morphology and function according to the site of maximum compression: effect of physical exertion and respiratory cycle. *Eur Heart J Cardiovasc Imaging* 2020;**21**:44–84.

34. Larsen CK, Aalen JM, Stokke C, Fjeld JG, Kongsgaard E, Duchenne J *et al.* Regional myocardial work by cardiac magnetic resonance and non-invasive left ventricular pressure: a feasibility study in left bundle branch block. *Eur Heart J Cardiovasc Imaging* 2020;**21**:143–53.

35. Agger P, Hyldebrandt JA, Hansen ESS, Omann C, Bøgh N, Waziri F *et al.* Magnetic resonance hyperpolarization imaging detects early myocardial dysfunction in a porcine model of right ventricular heart failure. *Eur Heart J Cardiovasc Imaging* 2020;**21**:93–101.

36. Attard MI, Dawes TJW, De Marvao A, Biffi C, Shi W, Wharton J *et al.* Metabolic pathways associated with right ventricular adaptation to pulmonary hypertension: 3D analysis of cardiac magnetic resonance imaging. *Eur Heart J Cardiovasc Imaging* 2019;**20**:668–76.

37. Nitsche C, Kammerlander AA, Binder C, Duca F, Aschauer S, Koschutnik M *et al.* Native T1 time of right ventricular insertion points by cardiac magnetic resonance: relation with invasive haemodynamics and outcome in heart failure with preserved ejection fraction. *Eur Heart J Cardiovasc Imaging* 2020;**21**:683–91.

38. Byrne C, Hasbak P, Kjær A, Thune JJ, Køber L. Myocardial perfusion during atrial fibrillation in patients with non-ischaemic systolic heart failure: a cross-sectional study using Rubidium-82 positron emission tomography/computed tomography. *Eur Heart J Cardiovasc Imaging* 2019;**20**:233–40.

39. Nielsen RR, Sörensen J, Tolbod L, Alstrup AKO, Iversen P, Frederiksen CA *et al.* Quantitative estimation of extravascular lung water volume and preload by dynamic 15O-water positron emission tomography. *Eur Heart J Cardiovasc Imaging* 2019;**20**:1120–8.

40. Ewen S, Karliova I, Weber P, Schirmer SH, Abdul-Khaliq H, Schöpe J *et al.* Echocardiographic criteria to detect unicuspid aortic valve morphology. *Eur Heart J Cardiovasc Imaging* 2019;**20**:40–4.

41. Kamphuis VP, Elbaz MSM, van den Boogaard PJ, Kroft LJM, van der Geest RJ, de Roos A *et al.* Disproportionate intraventricular viscous energy loss in Fontan patients: analysis by 4D flow MRI. *Eur Heart J Cardiovasc Imaging* 2019;**20**:323–33.

42. Grotenhuis HB, Cifra B, Mertens LL, Riessenkampff E, Manlhiot C, Seed M *et al.* Left ventricular remodelling in long-term survivors after the arterial switch operation for transposition of the great arteries. *Eur Heart J Cardiovasc Imaging* 2019;**20**:101–7.

43. Diller GP, Babu-Narayan S, Li W, Radojevic J, Kempny A, Uebing A *et al.* Utility of machine learning algorithms in assessing patients with a systemic right ventricle. *Eur Heart J Cardiovasc Imaging* 2019;**20**:925–31.

44. Gnanappa GK, Celermajer DS, Zhu D, Puranik R, Ayer J. Severe right ventricular dilatation after repair of Tetralogy of Fallot is associated with increased left ventricular preload and stroke volume. *Eur Heart J Cardiovasc Imaging* 2019;**20**:1020–6.

45. Rashid I, Mahmood A, Ismail TF, O'Meagher S, Kutty S, Celermajer D *et al.* Right ventricular systolic dysfunction but not dilatation correlates with prognostically significant reductions in exercise capacity in repaired Tetralogy of Fallot. *Eur Heart J Cardiovasc Imaging* 2020;**21**:906–13.

46. Cochet H, Iriart X, Allain-Nicolaï A, Camaioni C, Sridi S, Nivet H *et al.* Focal scar and diffuse myocardial fibrosis are independent imaging markers in repaired tetralogy of Fallot. *Eur Heart J Cardiovasc Imaging* 2019;**20**:990–1003.

47. Garg PK, Buzkova P, Meyghani Z, Budoff MJ, Lima J, Criqui M *et al.* Valvular calcification and risk of peripheral artery disease: the Multi-Ethnic Study of Atherosclerosis (MESA). *Eur Heart J Cardiovasc Imaging* 2019;**21**:1152–9.

48. Stella S, Italia L, Geremia G, Rosa I, Ancona F, Marini C *et al.* Accuracy and reproducibility of aortic annular measurements obtained from echocardiographic 3D manual and semi-automated software analyses in patients referred for transcatheter aortic valve implantation: implication for prosthesis size selection. *Eur Heart J Cardiovasc Imaging* 2019;**20**:45–55.

49. Visby L, Kristensen CB, Pedersen FHG, Sigvardsen PE, Kofoed KF, Hassager C *et al.* Assessment of left ventricular outflow tract and aortic root: comparison of 2D and 3D transthoracic echocardiography with multidetector computed tomography. *Eur Heart J Cardiovasc Imaging* 2019;**20**:1156–63.

50. Boraita A, Morales-Acuna F, Marina-Breysse M, Heras ME, Canda A, Fuentes ME *et al.* Bicuspid aortic valve behaviour in elite athletes. *Eur Heart J Cardiovasc Imaging* 2019;**20**:772–80.

51. Padang R, Enriquez-Sarano M, Pislaru SV, Maalouf JF, Nkomo VT, Mankad SV *et al.* Coexistent bicuspid aortic valve and mitral valve prolapse: epidemiology, phenotypic spectrum, and clinical implications. *Eur Heart J Cardiovasc Imaging* 2019;**20**:677–86.

52. Vollema EM, Singh GK, Prihadi EA, Regeer MV, Ewe SH, Ng ACT *et al.* Time course of left ventricular remodelling and mechanics after aortic valve surgery: aortic stenosis vs. aortic regurgitation. *Eur Heart J Cardiovasc Imaging* 2019;**20**:1105–11.

53. Szilveszter B, Oren D, Molnár L, Apor A, Nagy AI, Molnár A *et al.* Subclinical leaflet thrombosis is associated with impaired reverse remodelling after transcatheter aortic valve implantation. *Eur Heart J – Cardiovasc Imaging* 2019;**21**: 1144–51.

54. Saeed S, Vamvakidou A, Seifert R, Khattar R, Li W, Senior R. The impact of aortic valve replacement on survival in patients with normal flow low gradient severe aortic stenosis: a propensity-matched comparison. *Eur Heart J Cardiovasc Imaging* 2019;**20**:1094–101.

55. Kimura T, Roger VL, Watanabe N, Barros-Gomes S, Topilsky Y, Nishino S *et al.* The unique mechanism of functional mitral regurgitation in acute myocardial infarction: a prospective dynamic 4D quantitative echocardiographic study. *Eur Heart J Cardiovasc Imaging* 2019;**20**:396–406.

56. Ikenaga H, Makar M, Rader F, Siegel RJ, Kar S, Makkar RR *et al.* Mechanisms of mitral regurgitation after percutaneous mitral valve repair with the MitraClip. *Eur Heart J Cardiovasc Imaging* 2019;**21**:1131–43.

57. Pimor A, Galli E, Vitel E, Corbineau H, Leclercq C, Bouzille G *et al.* Predictors of post-operative cardiovascular events, focused on atrial fibrillation, after valve surgery for primary mitral regurgitation. *Eur Heart J Cardiovasc Imaging* 2019;**20**: 177–84.

58. Liu B, Edwards NC, Pennell D, Steeds RP. The evolving role of cardiac magnetic resonance in primary mitral regurgitation: ready for prime time? *Eur Heart J Cardiovasc Imaging* 2019;**20**:123–30.

59. Utsunomiya H, Itabashi Y, Kobayashi S, Yoshida J, Ikenaga H, Rader F *et al.* Comparison of mitral valve geometrical effect of percutaneous edge-to-edge repair between central and eccentric functional mitral regurgitation: clinical implications. *Eur Heart J Cardiovasc Imaging* 2019;**20**:455–66.

60. Brouwer HJ, Den Heijer MC, Paelinck BP, Debonnaire P, Vanderheyden M, Van De Heyning CM *et al.* Left ventricular remodelling patterns after MitraClip implantation in patients with severe mitral valve regurgitation: mechanistic insights and prognostic implications. *Eur Heart J Cardiovasc Imaging* 2019;**20**: 307–13.

61. Cimino S, Maestrini V, Cantisani D, Petronilli V, Filomena D, Mancone M *et al.* 2D/3D echocardiographic determinants of left ventricular reverse remodelling after MitraClip implantation. *Eur Heart J Cardiovasc Imaging* 2019;**20**:558–64.

62. Faletra FF, Leo LA, Paiocchi VL, Caretta A, Viani GM, Schlossbauer SA *et al.* Anatomy of mitral annulus insights from non-invasive imaging techniques. *Eur Heart J Cardiovasc Imaging* 2019;**20**:843–57.

63. Santoro C, Marco Del Castillo A, González-Gómez A, Monteagudo JM, Hinojar R, Lorente A *et al.* Mid-term outcome of severe tricuspid regurgitation: are there any differences according to mechanism and severity? *Eur Heart J Cardiovasc Imaging* 2019;**20**:1035–42.

64. Amano M, Izumi C, Taniguchi T, Morimoto T, Miyake M, Nishimura S *et al.* Impact of concomitant tricuspid regurgitation on long-termoutcomes in severe aortic stenosis. *Eur Heart J Cardiovasc Imaging* 2019;**20**:353–60.

65. Nassif M, Van Der Kley F, Abdelghani M, Kalkman DN, De Bruin-Bon R, Bouma BJ *et al.* Predictors of residual tricuspid regurgitation after percutaneous closure of atrial septal defect. *Eur Heart J Cardiovasc Imaging* 2019;**20**:225–32.

66. Faletra FF, Leo LA, Paiocchi VL, Schlossbauer SA, Borruso MG, Pedrazzini G *et al.* Imaging-based tricuspid valve anatomy by computed tomography, magnetic resonance imaging, two and three-dimensional echocardiography: correlation with anatomic specimen. *Eur Heart J Cardiovasc Imaging* 2019;**20**:1–13.

67. Koo HJ, Kang JW, Oh SY, Kim DH, Song JM, Kang DH *et al.* Cardiac computed tomography for the localization of mitral valve prolapse: scallop-by-scallop comparisons with echocardiography and intraoperative findings. *Eur Heart J Cardiovasc Imaging* 2019;**20**:550–7.

68. Dux-Santoy L, Guala A, Teixidó-Turà G, Ruiz-Muñoz A, Maldonado G, Villalva N *et al.* Increased rotational flow in the proximal aortic arch is associated with its dilation in bicuspid aortic valve disease. *Eur Heart J Cardiovasc Imaging* 2019;**20**:1407–17.

69. Hwang IC, Kim HK, Park JB, Park EA, Lee W, Lee SP *et al.* Aortic valve replacement-induced changes in native T1 are related to prognosis in severe aortic stenosis: T1 mapping cardiac magnetic resonance imaging study. *Eur Heart J Cardiovasc Imaging* 2020;**21**:653–63.

70. Mortensen KH, Wen J, Erlandsen M, Trolle C, Ringgaard S, Gutmark EJ *et al.* Aortic growth rates are not increased in Turner syndrome—a prospective CMR study. *Eur Heart J Cardiovasc Imaging* 2019;**20**:1164–70.

71. Van Der Ven JPG, Sadighy Z, Valsangiacomo Buechel ER, Sarikouch S, Robbers-Visser D, Kellenberger CJ *et al.* Multicentre reference values for cardiac magnetic resonance imaging derived ventricular size and function for children aged 0-18 years. *Eur Heart J Cardiovasc Imaging* 2020;**21**:102–13.

72. Pathan F, Zainal Abidin HA, Vo QH, Zhou H, D'Angelo T, Elen E *et al.* Left atrial strain: a multi-modality, multi-vendor comparison study. *Eur Heart J Cardiovasc Imaging* 2019;doi:10.1093/ehjci/jez303.

73. Truong VT, Palmer C, Wolking S, Sheets B, Young M, Ngo TNM *et al.* Normal left atrial strain and strain rate using cardiac magnetic resonance feature tracking in healthy volunteers. *Eur Heart J Cardiovasc Imaging* 2020;**21**:446–53.

74. Raisi-Estabragh Z, Izquierdo C, Campello VM, Martin-Isla C, Jaggi A, Harvey NC *et al.* Cardiac magnetic resonance radiomics: basic principles and clinical perspectives. *Eur Heart J Cardiovasc Imaging* 2020;**21**:349–56.

75. Van Hout MJP, Dekkers IA, Westenberg JJM, Schalij MJ, Scholte AJHA, Lamb HJ. The impact of visceral and general obesity on vascular and left ventricular function and geometry: a cross-sectional magnetic resonance imaging study of the UK Biobank. *Eur Heart J Cardiovasc Imaging* 2020;**21**:273–81.

76. Lim DJ, Ambale-Ventakesh B, Ostovaneh MR, Zghaib T, Ashikaga H, Wu C *et al.* Change in left atrial function predicts incident atrial fibrillation: the Multi-Ethnic Study of Atherosclerosis. *Eur Heart J Cardiovasc Imaging* 2019;**20**:979–87.

77. Anand SS, Tu JV, Desai D, Awadalla P, Robson P, Jacquemont S *et al.* Cardiovascular risk scoring and magnetic resonance imaging detected subclinical cerebrovascular disease. *Eur Heart J Cardiovasc Imaging* 2020;**21**:692–700.